Electronic Supplementary Material (ESI) for Inorganic Chemistry Frontiers.

Supporting information

Design of 3D alumina-doped magnesium oxide aerogels with high efficiency removal of uranium (VI) from wastewater

Yuqing Lei[a,b#], Keding Li[a#], Jun Liao[a], Yong Zhang [a*], Lin Zhang [b], Wenkun Zhu[a*]

[a] State Key Laboratory of Environment-friendly Energy Materials, Sichuan Co-Innovation Center for New Energetic Materials, National Co-innovation Center for Nuclear Waste Disposal and Environmental Safety, Nuclear Waste and Environmental Safety Key Laboratory of Defense, School of National Defence Science & Technology, Southwest University of Science and Technology, Mianyang 621010, China.

[b] Division of Target Science and Fabrication, Research Center of Laser Fusion, China Academy of Engineering Physics, P. O. Box 919-987, Mianyang 621900, P. R. China.

[#]Yuqing Lei and Keding Li contributed equally to this study.

[*]Corresponding author. E-mail: pandmzy@foxmail.com (Y. Zhang), zhuwenkun@swust.edu.cn (W. Zhu).

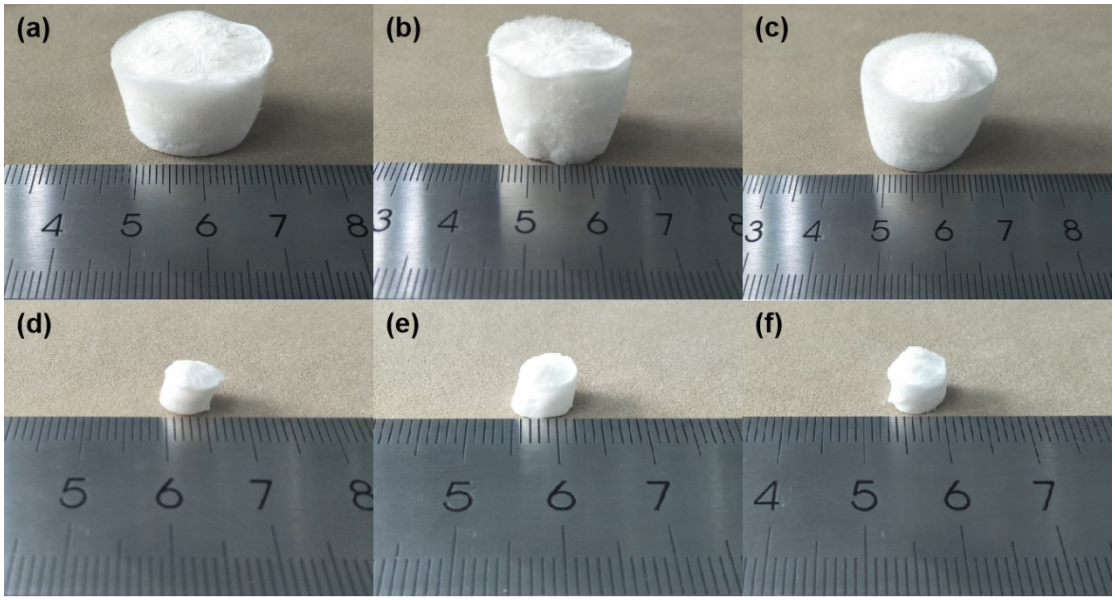

Figure S1. The optical images of (a) Al/Mg-N1, (b) Al/Mg-N2, (c) Al/Mg-N3, (d) Al/Mg-1, (e) Al/Mg-2 and (f) Al/Mg-3.

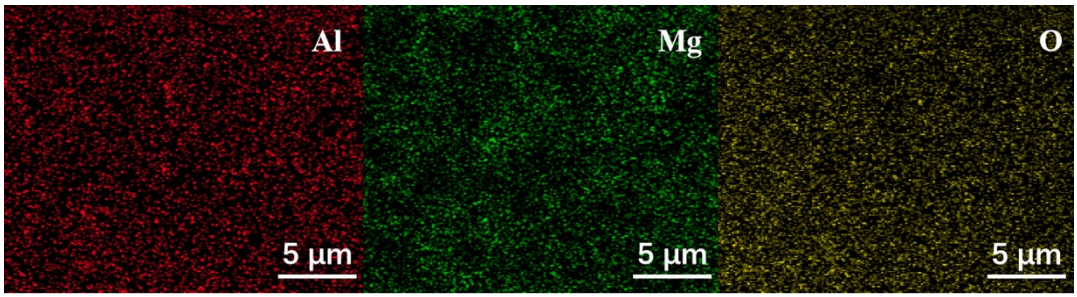

Figure S2. Elemental mapping of Al, Mg and O of Al/Mg-3.

Adsorption efficiency and adsorption capacity

Adsorption efficiency and adsorption capacity were the standards to measure the adsorption performance of adsorbents. The adsorption efficiency (%) and the adsorption capacity (q_e, mg·g^{-1}) of Al_2O_3/MgO aerogels for U(VI) were obtained by the following equations:

$$\text{Adsorption efficiency}(\%) = \frac{(C_0 - C_e)}{C_0} \times 100\% \quad \text{(S1)}$$

$$q_e = \frac{v \times (C_0 - C_e)}{m} \quad \text{(S2)}$$

Where C_0 (mg·L^{-1}) and C_e (mg·L^{-1}) were the initial and equilibrium concentrations of U(VI) in solution, respectively; v (L) was the volume of the solution; m (g) was the weight of adsorbents.

Adsorption kinetics

Pseudo-first-order and pseudo-second-order kinetic models

The adsorption kinetics of U(VI) on Al_2O_3/MgO aerogels were simulated by the pseudo-first-order kinetic model and the pseudo-second-order kinetic model, which corresponded to the physisorption behavior and chemisorption process between pollutants and adsorbents, respectively. The pseudo-first-order kinetic model (S3) and pseudo-second-order kinetic model (S4) were expressed as follows:

$$\ln(q_e - q_t) = \ln q_e - k_1 t \tag{S3}$$

$$\frac{t}{q_e} = \frac{1}{(q_e^2 \times k_2)} + \frac{t}{q_e} \tag{S4}$$

Where q_e (mg·g^{-1}) and q_t (mg·g^{-1}) were the equilibrium adsorption capacity and adsorption capacity at different time, respectively. k_1 (L·mg^{-1}) and k_2 (g·min^{-1}·mg^{-1}) were reaction rate constant of the pseudo-first-order and pseudo-second-order models, respectively. t (min) was the adsorption time of Al_2O_3/MgO aerogels.

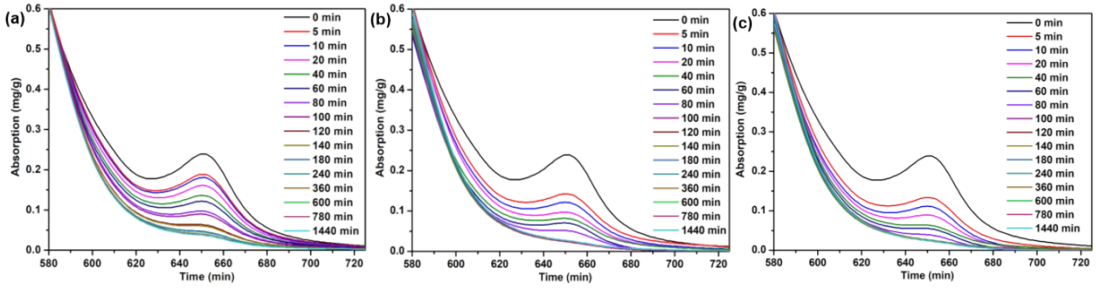

Figure S3. UV-vis absorption spectra of U(VI) adsorbed by Al_2O_3/MgO aerogels with Al_2O_3/MgO molar ratios of 1:0 (a), 2:1 (b) and 1:1 (c). All experiments were conducted at T = 25 °C, $C_{U(VI)}$ = 10 mg·L^{-1} and pH = 6.0.

Isotherm model

Langmuir and Freundlich adsorption isotherm models

The Langmuir adsorption isotherm model was used to describe the behavior of monolayer adsorption, while the Freundlich adsorption isotherm model was suitable for multilayer adsorption. They had been widely used isotherm in adsorption. The experimental data were analyzed by Langmuir (S5) and Freundlich (S6) sorption isotherm models, which were established as follows:

$$\frac{C_e}{q_e} = \frac{1}{q_m k_L} + \frac{C_e}{q_m} \tag{S5}$$

$$\ln q_e = \ln \mathrm{k}_F + \frac{1}{n} \ln C_e \tag{S6}$$

Where q_m (mg·g^{-1}) was the maximum adsorption capacity; k_L (L·mg^{-1}) was the the adsorption equilibrium constant of Langmuir; k_F (mg·g^{-1}) and n were the Freundlich constants associated with adsorption capacity and strength, respectively.

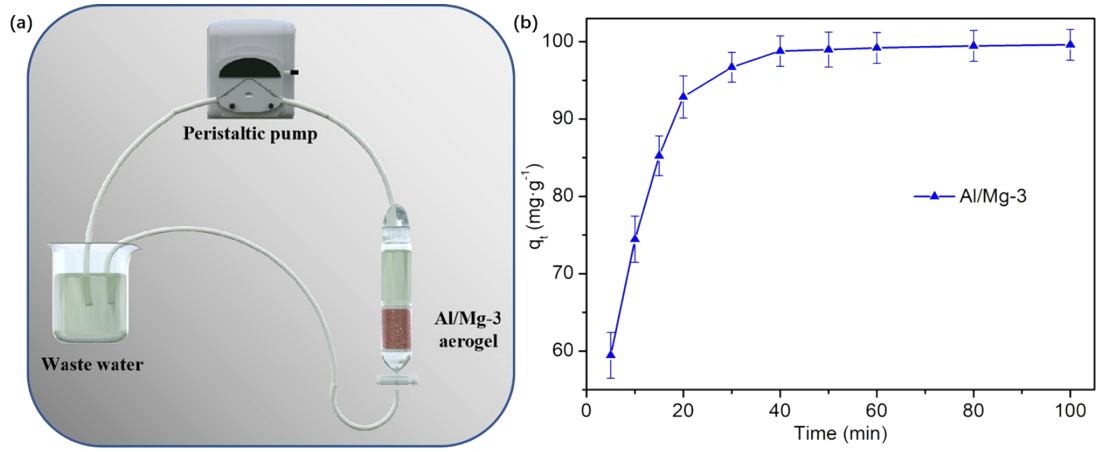

Figure S4. (a) Continuous U(VI) separation process of Al_2O_3/MgO aerogels with Al_2O_3/MgO molar ratios of 1:1 (Al/Mg-3). (b) Dynamic adsorption curves for U(VI) on Al/Mg-3, react time of 5-100 min.

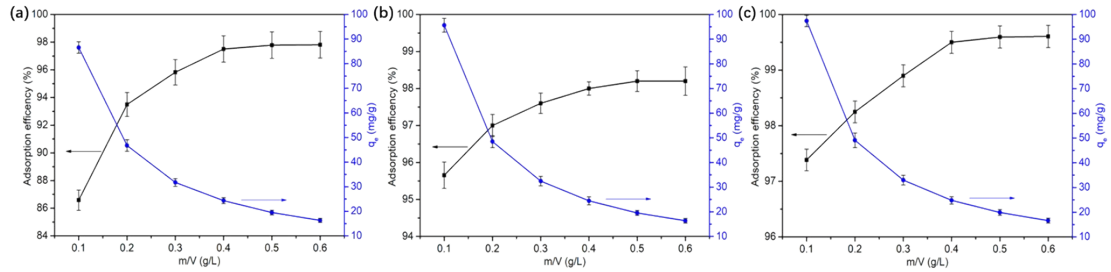

Figure S5. Effect of Al/Mg-1 (a), Al/Mg-2 (b) and Al/Mg-3 (c) content on the U(VI) adsorption. All experiments were conducted at T = 25 °C, $C_{U(VI)}$ = 10 mg·L^{-1} and pH = 6.0.

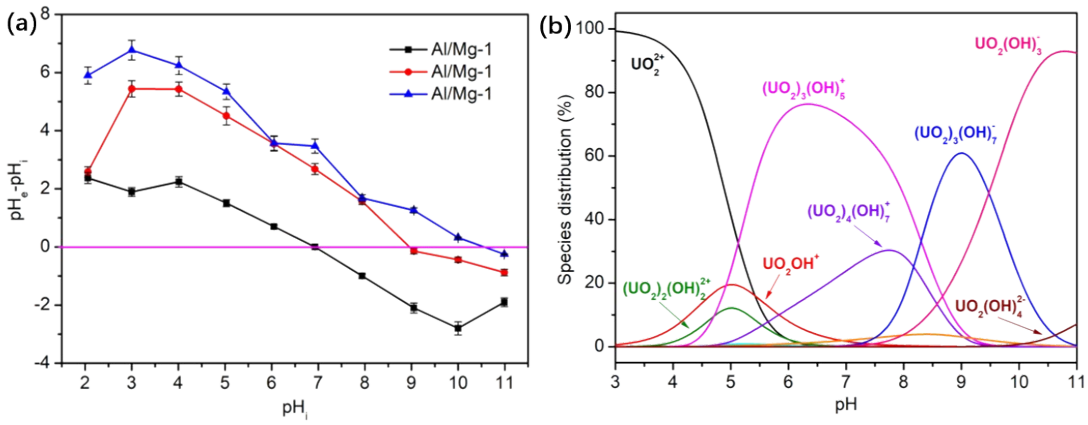

Figure S6. (a) Determination of pH_{ZPC} for the Al_2O_3/MgO aerogels with Al_2O_3/MgO molar ratios of 1:0 (Al/Mg-1), 2:1 (Al/Mg-2), 1:1 (Al/Mg-3). (b) Species distribution of U(VI) as a function of pH at $C_{U(VI)}$ = 10 mg·L^{-1} and T = 25 °C.

Table S1 Physical parameters of Al_2O_3/MgO aerogels with Al_2O_3/MgO molar ratios of 1:0 (Al/Mg-1), 2:1 (Al/Mg-2), 1:1 (Al/Mg-3).

Sample	Density ($mg \cdot cm^{-3}$)		
	Before calcination	After calcination	Increased density
Al/Mg-1	9.42	28.89	19.47
Al/Mg-2	12.10	21.33	9.23
Al/Mg-3	13.12	18.89	5.77

Table S2 The mass and atomic percentage of each element in Al/Mg-3.

Element	Weight (%)	Atomic (%)
Al	38.01	28.57
Mg	16.91	14.29
O	45.08	57.14
Totals	100.00	100.00

Table S3 The static adsorption and dynamic adsorption of uranium(Ⅵ) solution by Al_2O_3/MgO aerogels with Al_2O_3/MgO molar ratios of 1:1 (Al/Mg-3).

Samples	Pollutant	Static absorption		Continuous adsorption	
		q_e (mg·g^{-1})	Adsorption efficiency (%)	q_e (mg·g^{-1})	Adsorption efficiency (%)
Al/Mg-3	U(VI)	97.2	97.2	99.6	99.6

Table S4 The actual adsorption capacity of Al_2O_3/MgO aerogels for different concentrations of U(VI).

Concentration ($mg \cdot L^{-1}$)	Adsorption capacity ($mg \cdot g^{-1}$)		
	Al/Mg-1	Al/Mg-2	Al/Mg-3
5	44.8	47.0	47.0
10	93.1	92.6	97.7
20	195.7	188.5	189.2
40	287.6	332.9	375.2
60	362.5	433.4	530.3
80	404.3	515.3	662.0
100	447.9	562.3	771.1
120	472.9	601.0	836.5
150	497.1	636.5	900.3
200	518.0	670.7	958.1